I CRISTALLI SONICI COME BARRIERE ANTIRUMORE

SONIC CRYSTALS AS TUNABLE NOISE BARRIERS

Federica Morandi * (1), Alessandro Marzani (2), Simona De Cesaris (3), Dario D'Orazio (1), Luca Barbaresi (1), Massimo Garai (1)

1) Dipartimento di Ingegneria Industriale, Università di Bologna, Bologna
2) Dipartimento di Ingegneria Civile, Chimica, Ambientale e dei Materiali, Università di Bologna, Bologna
3) Magneti Marelli S.p.A.

* Indirizzo dell'autore di riferimento - Corresponding author's address:
Viale del Risorgimento 2, 40136, Bologna, Italia
e-mail: federica.morandi6@unibo.it

RIASSUNTO

Il presente contributo riporta un'introduzione al tema della propagazione del suono nei cristalli sonici e un excursus sulla letteratura scientifica più recente. Si discutono i risultati di alcune indagini sperimentali condotte presso l'Università di Bologna inerenti misure di Insertion Loss, misure effettuate all'interno del reticolo e misure di intensimetria. Infine i valori di Sound Insulation misurati per un cristallo sonico sono confrontati con valori misurati su barriere tradizionali, evidenziando come il cristallo sonico permetta di raggiungere un isolamento confrontabile con il valore soglia di Insertion Loss raggiungibile a causa della diffrazione del bordo superiore della barriera.

ABSTRACT

This work reports an introduction to the topic of wave propagation in sonic crystals and a review of the recent scientific literature. The paper presents the results of some experimental investigations carried out at the University of Bologna by discussing Insertion Loss measurements, measurements performed inside the lattice and sound intensity measurements. Finally, the Sound Insulation Index measured for a sonic crystal is compared to the values measured for common noise barriers, pointing out that sonic crystals reach insulation values comparable to the maximum Insertion Loss achievable due to the top edge diffraction.

Federica Morandi et al.
I cristalli sonici come barriere antirumore
Sonic crystals as tunable noise barriers

1. Introduzione

Wave propagation through periodic media is a research field that, starting from the solid state physics, drew the attention of the research in many areas; in the last fifteen years acoustics has been one of the most promising sectors.

The first studies of wave propagation in periodic structures relates to the propagation of electromagnetic waves in solids [1]. From the late 80's it became clear that also classical waves supported the phenomenon of band structures and pioneering works investigated the propagation of electromagnetic waves in media with periodically-modulated refractive indices [2], opening the research field of photonic crystals [3]. An increase in attention on elastic band gap materials produced a wide literature on the so-called phononic crystals, i.e. inhomogeneous elastic media composed of n-dimensional periodic arrays of inclusions embedded in a matrix [4]. Band structures analysis for elastic media have been investigated theoretically and numerically with methods spanning from multiple scattering formulations to the plane wave expansion [5-7].

A great stimulus to the development of studies on periodic media was due to the first experimental measurements on metamaterials. The first theoretical reference to metamaterials dates back to 1968, when Veselago [8] investigated theoretically the properties of materials where the real part of the electric permittivity and magnetic permeability are simultaneously negative, resulting thus in a negative refractive index. He anyway could not demonstrate experimentally the consequences he predicted as he could not get any material to assume a negative permeability. More than 30 years after, composite media displaying simultaneously negative permeability and permittivity brought the first experimental evidence of Veselago's intuitions [9, 10].

In recent years many works investigated metamaterials for acoustic applications, the milestone being the work by Liu et al [11]. The strong periodic modulation of density and/or sound velocity forbids wave propagation at certain frequencies in the long wavelength limit, i.e., in the spectral regions corresponding to wavelengths much larger than the size of the inhomogeneities. Below the homogenization limit, the medium can be considered as homogeneous and theories related to composite medium hold, i.e. properties such as density and bulk modulus are correlated to the emerging properties of the composite material. This is the reason why negative densities and bulk moduli occur, which would not be conceivable for non-composite materials. One of the most interesting properties of such metamaterials is that they proved to be effective at low frequency as they break the mass law and provide significant acoustic attenuation even in reduced thicknesses. The literature produced significant experimental proofs related to acoustic metamaterials displaying negative density, negative bulk modulus or a combination of the two [12–18].

The study of engineered composite materials also gave rise to a research field related to cloaking. The original idea is that since Maxwell equations are invariant for a coordinate change, it is possible to use singular transformations to achieve cloaking of the electromagnetic waves [19, 20]. In recent years Milton [21] transposed this concept to the equations of motion for a general elastic medium but found out that, in general, they are not invariant to coordinate transformation. Cummer et al. [22] showed that in two dimensions, where the equivalence between electromagnetics and elastodynamics holds, the coordinate transformation holds also for anisotropic media, opening a way to acoustic cloaking [23].

Federica Morandi et al.
I cristalli sonici come barriere antirumore
Sonic crystals as tunable noise barriers

2. Sonic crystals: from the origins to the state of art

2.1 The formation of band structures in sonic crystals

Sonic crystals are arrangements of scatterers immersed in air. In the space domain, a direct lattice, or Bravais lattice, is defined as an infinite set of points generated by the translation of a set of vectors which are linearly independent. The physical arrangement of the whole crystal can be defined by specifying the contents of a single unit cell, whose repetition following the primitive vectors generates the crystal structure. The reciprocal lattice is defined together with the direct lattice; it is the set of vectors in the Fourier space that give plane wave with the same periodicity of the direct lattice. As wave functions are periodic in the direct lattice, the solutions in the Fourier space are periodic in the reciprocal lattice, and as well as calculation in the direct lattice are constrained to the unit cell, in the reciprocal lattice calculations are constrained to the first Brillouin zone. Each unit cell is characterized by a lattice constant and a filling fraction. The lattice constant is a parameter related to the physical dimension of the unit cell while the filling fraction is the ratio of the volume occupied by the scatterer to the volume of the whole unit cell.
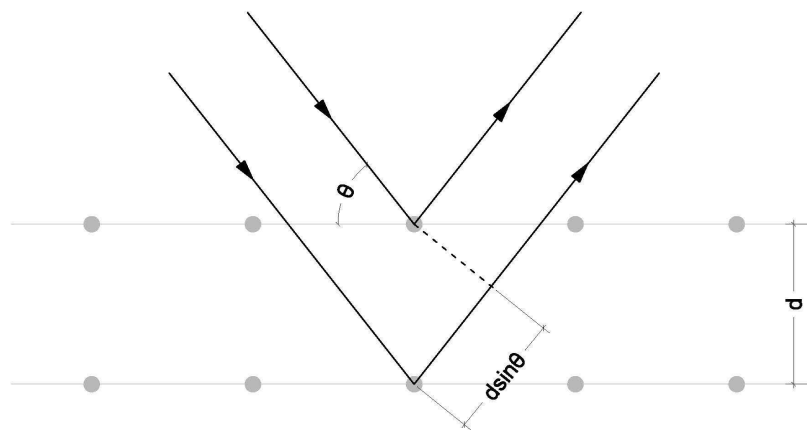

Figure 1 - Lo scattering di Bragg - Bragg scattering.

In 1913 Bragg gave an effective explanation to the observed angles of diffracted beams from a crystal. He observed that for certain incidence angles and wavelengths the intensity of the reflected beams was strenghtened. Whenever the path difference for rays reflected from adjacent planes is an integer number of the incident wavelength, the reflections from all parallel planes add up in phase giving a strong reflected beam. This condition can be formulated as:

(1)
$$2d \sin(\vartheta) = n\lambda$$

where d the distance between two adjacent planes of a lattice (Fig. 1). The frequency for which this condition is met is generally referred to as Bragg frequency, and for normal incidence it takes the form: $f_{Bragg} = c/2d$, c being the speed of sound in air.

Even though the physical problem that lies beyond Bragg formulation (atoms placed in a periodic potential) is totally different from the problem of scatterers immersed in air

Federica Morandi et al.
I cristalli sonici come barriere antirumore
Sonic crystals as tunable noise barriers

some conclusions still hold; therefore an analogy can be formulated. Assuming a harmonic temporal dependence, the wave equation in free field

$$(2) \qquad (\nabla^2 + k^2)p = 0$$

has a solution of the type $e^{i\vec{k}\vec{x}}$, where $\vec{k}$ is the wave vector. In a periodic medium, one will have to solve

$$(3) \qquad (\nabla^2 + k^2)p_k = 0$$

with the periodic condition (Bloch-Floquet theorem):

$$(4) \qquad p_k(\vec{r} + \vec{R}) = p_k e^{i\vec{k}\vec{R}}$$

where $\vec{R}$ is a vector of the direct lattice and $\vec{k}$ represents the wave vector inside the periodic medium and its values lie within the first Brillouin zone. Since in a 2D periodic medium the eigenvalue problem is restricted to a single unit cell, the eigenvalues $\omega(k)$ form a set of discrete frequencies which represent the frequencies supported by the lattice. Thus, for each value of wave number k there is an infinite set of modes with discretely spaced frequencies, which can be labeled by a band index n. Since k enters as a continuous parameter, we expect that the frequency of each band, for each n, varies continuously as k varies. The band structures thus are a set of continuous functions $\omega_n(k)$ indexed in order of increasing frequency by the band number [3].

The relation between ω and k is usually referred to as dispersion relation, and in the free field the proportional constant is the speed of sound, $c = \omega/k$. The flattening of the dispersion curves can be thought as a decrease of the speed of sound inside the crystal. Since the periodicity of the medium in general depends on the direction of propagation, the dispersion curves are usually represented in direction-dependent diagrams. For a 2D square lattice, the frequencies at which Bragg scattering occur are determined for normal incidence (ΓX direction) and for an incidence angle of 45° (ΓM direction) from:

$$(5) \qquad \nu_{\Gamma X} = \frac{c_{sound}}{2 \cdot L_c}, \qquad\qquad \nu_{\Gamma M} = \frac{c_{sound}}{2\sqrt{2} \cdot L_c}$$

At Bragg frequency, i.e. at the boundary of the 1st Brillouin zone, a standing wave is formed inside the crystal due to the interaction of the incident and the back-scattered wave. Since standing waves have null group velocity, $v_g = \partial\omega/\partial k = 0$, the dispersion curves will assume a horizontal tangent moving towards the boundaries of 1st Brillouin zone, leading to the opening of a band gap. The envelope of the standing wave which is formed at Bragg frequency displays a maximum in between the scatterers, i.e. where the material with higher sound propagation velocity lies. Thus, for the same wave number, two different frequencies are possible due to the different sound propagation velocities inside the two media. The width of the band gaps depends on the difference in velocity. Band

Federica Morandi et al.
I cristalli sonici come barriere antirumore
Sonic crystals as tunable noise barriers

structures are thus the solutions of the eigenvalue problem plotted in direction-dependent diagrams.
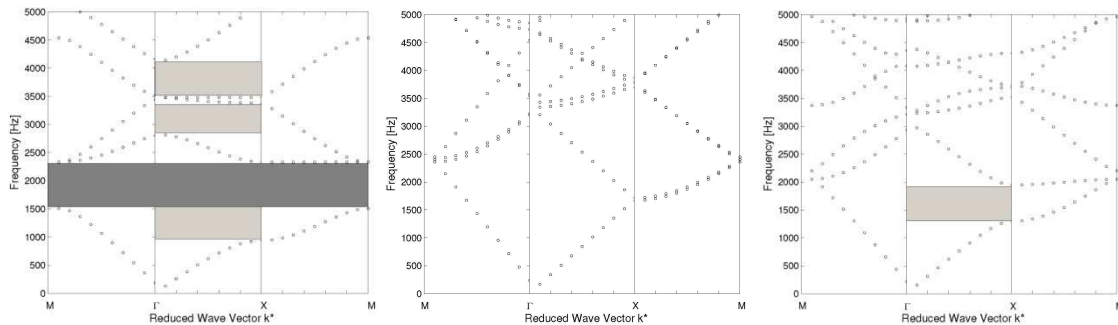

Figure 2 - Curve di dispersione calcolate con il metodo PWE per tre distinti reticoli quadrati di cilindri immersi in aria; la costante di reticolo è L_c=0.1 m e la filling fraction è ff=0.01 (a), ff=0.2 (b), ff=0.6 (c) - Dispersion curves extracted using the PWE method for three different square arrays of cylinders immersed in air; the lattice constant is L_c=0.1 m and the filling fraction is ff=0.01 (a), ff=0.2 (b), ff=0.6 (c).

Stop band phenomena occur when the sonic crystal shows a certain filling fraction. Fig. 2 depicts three band structures, for a square lattice of circular scatterers in 2D, i.e. an array of cylinders in 3D, calculated for a lattice constant Lc=0.10 m, where the first Bragg band gaps are expected at 1720 Hz for normal incidence (ΓX direction) and at 1210 Hz for an incidence angle of 45° (ΓM direction). Three filling fractions are considered, 0.01, 0.2, 0.6 which implies, leaving the lattice constant unchanged, the radii of the cylinders to be 0.0056, 0.0252 and 0.0437 m respectively. The x-axis reports the reduced wave vector k, while y-axis reports the frequency. If the filling fraction is small, as in Fig. 2 (a), the wave propagation inside the crystal is not affected by the presence of the scatterers and the dispersion relation assumes linear values, according to the law k=ω/c. Increasing the filling fraction to 0.2, Fig. 2 (b), a band gap opens in the ΓX direction (dark grey shade), centered around the Bragg frequency calculated above. With a filling fraction of 0.6, Fig. 2 (c), the band gap in the ΓX direction increases in width and band gaps open also for the ΓM and XM directions (light grey shade), leading to the formation of a complete band gap.

There exist five 2D lattices and fourteen 3D lattices; among the different 2D lattices (square, hexagonal, rectangular, oblique, and centered rectangular), the hexagonal showed to have the best insulation performance.

2.2 Literature review in brief

The first formulation of multiple scattering specifically tailored for cylinders arranged in air dates back to 1950, with the publication of the milestone work by Twersky [24] but the first experimental evidences of band gaps in sonic crystal date back only to 1995, when Martínez et al. [25] measured sound attenuation across a sculpture by Eusebio Sempere, exhibited outside the Juan March Foundation in Madrid. The sculpture basically consists of an arrangement of steel cylinders in air mounted on a circular platform. Measurements at different incidence angles provided the first evidences of the formation of acoustic band gaps in periodic elastic media [5]. After this

Federica Morandi et al.
I cristalli sonici come barriere antirumore
Sonic crystals as tunable noise barriers

pioneering work, several studies reported measurements and theoretical approaches to characterize sonic crystals. Tests involved the variation of the spatial arrangement of the cylinders and of the filling fraction, showing that simple lightweight sonic crystals are capable to reduce sound transmission up to 25 dB [26–29]. Closely related to the sound attenuation provided by sonic crystals are the reflectance properties of such periodic arrangements. Sanchis et al. [30] investigated the sound pressure field reflected from the sonic crystal by means of multiple scattering formulations which were verified by measurements. They found out that the standing wave ratio is enhanced in the same frequency range in which stop-band phenomena occur. The reflectance properties were further investigated and related to the band structures of the sonic crystal [31]. Though the early theoretical formulations of multiple scattering phenomena refer to rigid circular cylinders, other kind of scatterers have been analyzed in the literature. In particular, square scatterers rotated along the vertical plane have been investigated leading to a modeling of negative refraction [32] and to the optimization of tunable acoustic waveguides [33].

The most limiting property of sonic crystal is that stop-bands are constrained to a narrow band; thus an extensive literature focused on widening the frequency range of attenuation by associating separate attenuation mechanisms to Bragg scattering. The infinite possibilities of combination of these phenomena gave rise to several design optimized to provide a broadband attenuation. For instance, Romero et al. [34] designed an array of scatterers characterized by multiple resonances of different nature and material with different mechanical properties and geometries which provide attenuation effects in the long wavelength limit. Similarly, Elford et al. [35] proposed matryoshka resonant sonic crystals, i.e. concentric configurations of slotted cylinders that provide sound attenuation below Bragg frequency. Krynkin et al. proved that the periodic concentric arrangement of cylinders with slits and inner elastic shells provided attenuation below the first Bragg band gap [36]. Another solution to render sonic crystals effective broadband is the application of sound absorbing materials to the scatterers. Umnova et al. [37] provided theoretical and experimental evidences about the benefits achievable by the adding porous materials to the cylinders. Sánchez-Dehesa et al. [38] tested sonic crystals consisting of cylinders arranged in three layers and filled with rubber crumb. Sound attenuation was tested in an anechoic chamber and compared to the attenuation provided by plain rigid cylinders. García-Chocano et al. [39] performed measurement on the same two configurations measured in transmission chambers, i.e. in a diffuse field.

The application of sonic crystals as noise barrier was further developed by studying the effect of the ground where the scatterers are fixed and its interfering behavior with respect to the formation of band gaps. Kryinkin et al. [40] combined the effects of a two-dimensional (semi-infinite) periodic array of cylinders and a impedance ground where cylinders would be installed. The theoretical and experimental analysis showed that, while a rigid ground would mine the positive IL related to Bragg band gap, an impedance ground shifts the ground effect minima to lower frequencies, not interfering with the Bragg band gap. With a specific attention towards sustainable application as noise barriers, works have been devoted to quantify the attenuation produced by trees arranged in a periodic lattice [41] and by bamboo rods [42], both plain and drilled in order to couple resonance phenomena.

The inclusion of defects into sonic crystals has also been investigated, where these anomalies were for instance due to vacancies or modification of the dimensions of some scatterers [43, 44]. Evolutionary algorithms have been developed within the multiple

Federica Morandi et al.
I cristalli sonici come barriere antirumore
Sonic crystals as tunable noise barriers

scattering theory to allow a controlled manipulation of waves inside the sonic crystal by introducing vacancies in the lattice [45]. The evanescent behavior of modes in the band gap has been theoretically and experimentally demonstrated in the presence of lattice defects as well [46].

Some comprehensive works included many of the features exposed above, both in terms of design of the scatterers and measurement setup. One amongst all, Castineira-Ibánez et al. [47] characterized acoustic barriers based on fractal geometries to maximize the Bragg scattering and multi-phenomena scatterers with several noise control mechanisms, as resonances or absorption, by acoustic standardization tests according to EN 1793- 2 [48], i.e. under diffuse field conditions.

Sonic crystals with a low filling fraction were tested in a impedance tube in order to determine the reflection and absorption coefficient of sonic crystals below the homogenization limit [49]. By tuning the width of the cavity below the sample, the authors measured an absorption coefficient up to 0.8.

2.3 Theoretical models

Three methods are generally used to investigate sonic crystals and to support the experimental evidences: the Plane Wave Expansion method, (PWE), the Multiple Scattering Theory (MST) and the Finite Element (FE) method.

The Plane Wave Expansion method is based on the solution of the wave equation by applying Bloch-Floquet theorem and expanding the properties of the media in Fourier series [5]. In its basic formulation, it allows to calculate the band structure of the medium. The PWE medium can be applied to arrays of any kind of scatterers but only infinite arrays can be modeled. Local defects can be investigated using the PWE with the supercell approximation.

The Multiple Scattering Theory is a formulation that computes the pressure field as a sum of the multiple scattering process [50, 37]. It generates when a wave impinging on a scatterer produces a scattered wave which in turn is scattered by the other scatterers and so on. The implementation of this methods allows to compute the sound field generated by any array and no constrain on the periodicity or regularity of the array is required. Multiple scattering formulations can also be used to compute the band structures of periodic acoustic composites [7, 51].

The Finite Element method is a numerical method to solve partial differential equations. The domain is discretized into small regions in which the differential equations are approximately solved. This meshing procedure allows to describe also complex geometries. This method is not widely used in acoustic scattering problems due to the computational costs and to its intrinsic difficulty to cope with unbounded domains. PMLs or NRBCs can be used to emulate Sommerfeld's radiation conditions at infinity but still present critical issues when dealing with plane waves for boundaries normal to the wave vector of the travelling wave. It is though a robust method to calculate sound pressure fields through sonic crystals and can be used in combination with other programs to calculate the band structure of a given array.

Recently a method has been developed [52] that is based on the Method of Fundamental Solutions formulated in the frequency domain. Solving a 3-dimensional problem as a discrete summation of 2-dimensional problems, the authors could determine the sound field scattered by sonic crystals reducing dramatically the computational costs if compared to the Finite Element Method or the Boundary Element Method.

Federica Morandi et al.
I cristalli sonici come barriere antirumore
Sonic crystals as tunable noise barriers

3. Experimental measurements

3.1 The sound field across sonic crystals

The Acoustic Laboratory of the University of Bologna is a large industrial hall with a volume of about 5,000 m^3 currently used to test noise barriers according to the standards EN 1793-5 [53] and EN 1793-6 [54]. Measurements were performed over a 3 x 3 m sample consisting of PVC pipes 3 m long, with an outer diameter of 0.16 m and a thickness of 3.2 mm. The cylinders were arranged in a 15 x n square lattice, where n varied from 2 to 5. The lattice constant was Lc=0.20 m and has been chosen to test a configuration which could be effective for traffic noise; Bragg scattering occurs at 860 Hz, i.e. close to the maximum of the normalized tyre/road noise spectrum [55].

Figure 3 - Allestimento della catena di misura presso il Laboratorio di Acustica dell'Università di Bologna - Measurement setup at the Acoustic Laboratory of the University of Bologna.

The cylinders were fixed to the ground by means of a stratified board (plywood, plasterboard and polyester) and the top ends were fixed by some aluminum profiles. The source and the microphone were set at an height of 1.5 m from the ground, half the height of the sample, the microphones lying on the vertical axis. Figure 3 displays the measurement setup inside the facility.

Since measurements were performed in a laboratory and no impulsive background noises were present, Impulse Response (IR) measurements were performed using 128k Exponential Sine Swept (ESS) test signals sampled at 44.1 kHz, which were proved to be better suited in these conditions [56].

In the field of sonic crystals studies, the sound field is often characterized by the Insertion Loss (IL), defined as:

Federica Morandi et al.
I cristalli sonici come barriere antirumore
Sonic crystals as tunable noise barriers

(6)
$$IL = -20\log_{10}\frac{p_w}{p_{w/o}} \qquad (dB)$$

where p_w is the pressure field measured with the sample between source and receiver and $p_{w/o}$ is the pressure field measured in the same points without the sample. When the receiving microphone is on the rear side of the sonic crystal, this IL is equivalent to a transmission loss; when the microphone is on the front (source) side this IL is equivalent to a reflection factor on a logarithmic scale.

To characterize sound transmission through the sample, the source was set at a distance of 1 m from the closest cylinder, pointing at the centre of the array. The microphone was placed on the opposite side of the sample, at a distance of 0.25 m. Three measurement positions were tested, spaced apart by 1/4 of the lattice constant, and the sound source was shifted along the sample accordingly, in order to keep the source/receiver alignment. In position (a) the microphone and the sound source faces the centre of a cylinder; in position (c) the microphone faces the interstice between two adjacent cylinders and position (b) is intermediate between the two.

Sound reflection was evaluated by placing the sound source at a distance of 1.5 m from the sample and the microphone at a distance of 0.25 m from the sample, on the same side of the sound source. Measurements were performed on three measurement positions as well, respectively a, b and c.
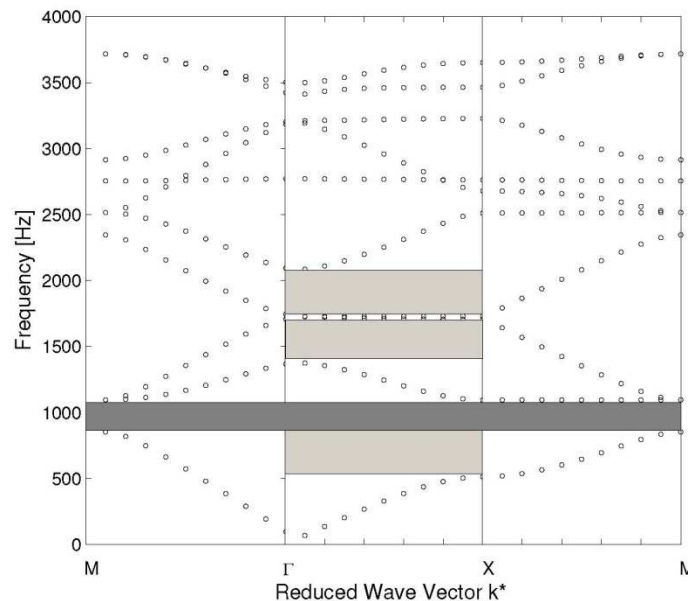

Figure 4 - Curve di dispersione per un reticolo quadrato di cilindri con Lc=0.20 m e r=0.08 m calcolate con il metodo PWE - Dispersion curves for a square array of cylinders with Lc=0.20 m and r=0.08 m evaluated using the PWE method.

The dispersion curves of the array (Lc=0.200 m and ff =0.50) are reported in Fig. 4. The first Bragg band gaps are expected at $f_{Bragg,\Gamma X}$=858 Hz for normal incidence and at $f_{Bragg,\Gamma M}$=606 Hz for an incidence angle of 45°. The band structures calculated with the PWE method spot a complete band gap in the range 850-1100 Hz. In the ΓX direction,

Federica Morandi et al.
I cristalli sonici come barriere antirumore
Sonic crystals as tunable noise barriers

the width of the band gap is greater and goes down to 520 Hz. A second band gap is clearly visible on ΓX in the range 1370-2090 Hz.

In order to investigate the effect of the addition of multiple layers of cylinders, sound insulation and reflection properties have been measured by varying the depth of the sample from 2 to 5 rows of cylinders [57, 58]. The IRs were windowed using a modified Adrienne time window made of (i) a leading edge having a left-half Blackman-Harris shape and a total length of 0.5 ms; (ii) a flat portion having a total length of 4.26 ms; (iii) a trailing edge having a right-half Blackman-Harris shape and a total length of 1.74 ms. In each configuration, the relative distance between the sound source, the sample and the microphone was kept the same, and so was the time window applied to the IRs, whose length is determined upon the cancellation of ground reflection and diffraction. The IL measured in insulation and reflection is reported in Fig. 5 for sonic crystals made of 2 and 3 rows of cylinders and for the three measurement positions mentioned above.
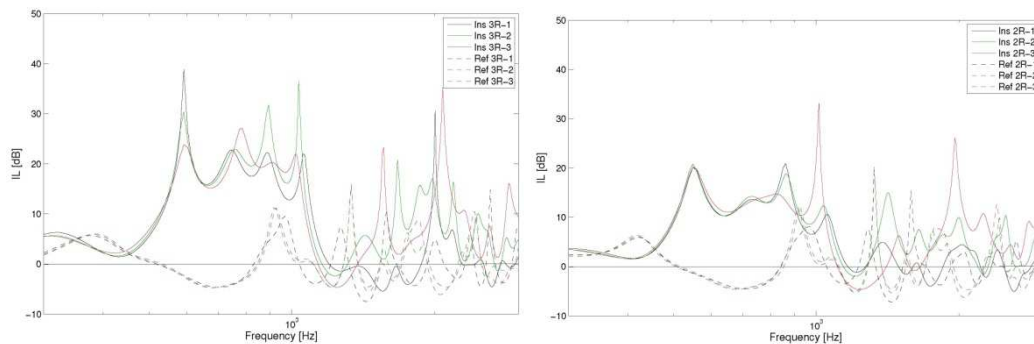

Figure 5 - Insertion Loss (dB) misurato in trasmissione (linea continua) ed in riflessione (linea tratteggiata) per un cristallo sonico costituito rispettivamente da 2 (a) e 3 (b) file di cilindri - Insertion Loss (dB) measured in transmission (solid line) and in reflection (dashed line) for a sonic crystal made of 2 (a) and 3 rows of cylinders (b).

Insertion Loss in transmission displays values up to 25 dB at Bragg frequency for a 3-rows sonic crystal, while IL measured in reflection reaches the values of zero, i.e. the sound energy incident on the sample is totally reflected. At higher frequencies, the behavior of the sample depends significantly on the microphone position. It is to notice that positive IL values in transmission correspond to (slightly) negative IL values in reflection, pointing out a phenomenon of constructive interference.

3.2 The sound field inside sonic crystals

In order to verify the scattering process occurring inside sonic crystals, a set of measurements has been conducted by placing the microphone inside a 3-rows sonic crystal and moving it along the transverse (SWT) and longitudinal (SWL) directions with a spacing of 1/4 of the lattice constant.

The results of the measurements inside the sonic crystals are reported in Fig. 6 on a flattened 3D graph, having position and frequency on the x- and y-axis respectively and Insertion Loss on the z-axis. A cubic interpolation was made over the y-axis (position) in order to smooth the surface and ease the understanding of the plot.

Federica Morandi et al.
I cristalli sonici come barriere antirumore
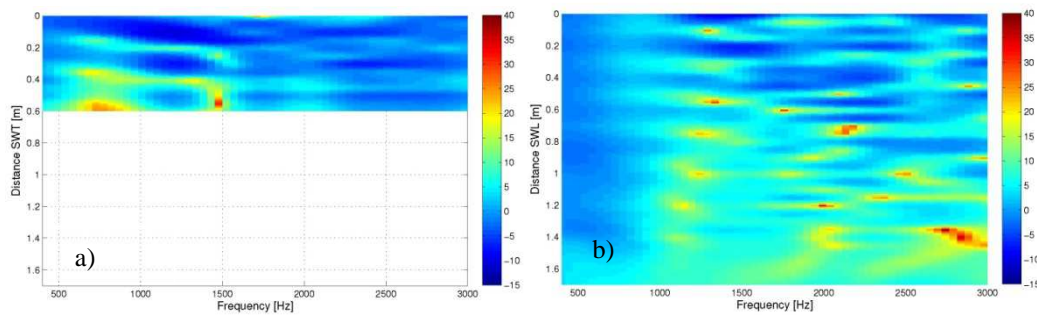**Sonic crystals as tunable noise barriers**

Figure 6 - Insertion Loss (dB) misurato all'interno del cristallo sonico nelle direzioni trasversale (a) e longitudinale (b). Frequenza sull'asse x, spostamento all'interno del cristallo sull'asse y - Insertion Loss (dB) measured inside the sonic crystal in the transverse (a) and longitudinal (b) directions. Frequency on the x-axis, displacement inside the crystal on the y-axis.

In the transverse direction, the Bragg band gap in the ΓX direction is clearly detected around 800 Hz and at twice that frequency. Moving away from the source, both the maxima and the minima of the IL increase, behavior which is related to the exponential decay of the evanescent mode inside the band gap [46]. After Bragg frequency, a region occurs in which the field is determined by constructive interference (negative IL) that repeats according to the Bloch-Floquet theorem with the periodicity of the crystal.

In the longitudinal direction a similar pattern occurs. An increase in IL is visible at around 800 Hz and a second region of positive IL appears at slightly higher frequencies, and shifts to lower frequencies moving away from the source. This phenomenon is due to the fact that as the microphone shifts all along the crystal away from the source, the periodicity of the crystal increases, and as a consequence Bragg frequency shifts towards lower frequencies.

3.3 Sound intensity measurements

It is a long debated topic whether there is any part of the sound field which travels in the longitudinal direction of sonic crystals. In order to evaluate the entity of sound emission from the side and front of the sample, sound intensity measurements were conducted on a 3-rows sonic crystals with the lattice properties discussed above.

The sound source was placed at a distance of 1 m from the sonic crystal and the intensity probe at a distance of 0.5 m. The resolution chosen is of two measurement positions per lattice constant, i.e. two consecutive measurement points are spaced apart by 0.10 m, and the probe was placed at three different heights: 1.4 m, 1.5 m and 1.6 m. In the following, only the measurements performed at a height of 1.5 m are presented. Fig. 7 shows the measurement setup. In order to minimize the effects of lateral diffraction and of the direct component, absorbing material was placed on the sides of the barrier.

Federica Morandi et al.
I cristalli sonici come barriere antirumore
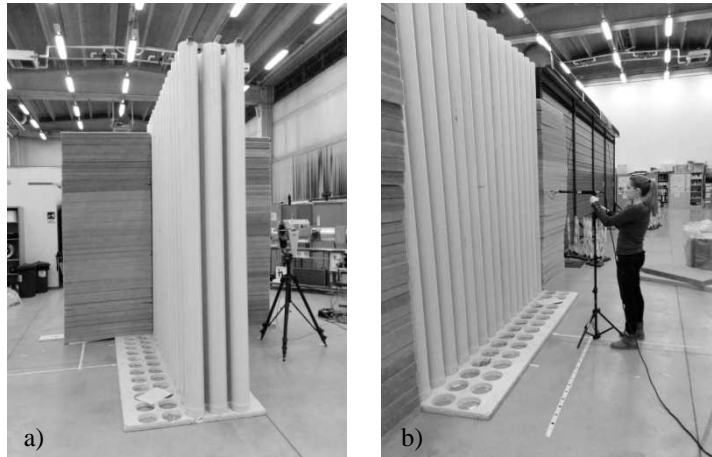**Sonic crystals as tunable noise barriers**

Figure 7 - Misure intensimetriche sul lato (a) e sul retro (b) del cristallo sonico - Sound intensity measurement setup on the side (a) and the rear (b) of the sonic crystal.

The results are reported as contour maps, where sound intensity and sound pressure levels are interpolated along the "side" and "back" displacement axes in one-third of octave bands ranging from 200 to 3150 Hz (Fig. 8 and Fig. 9).
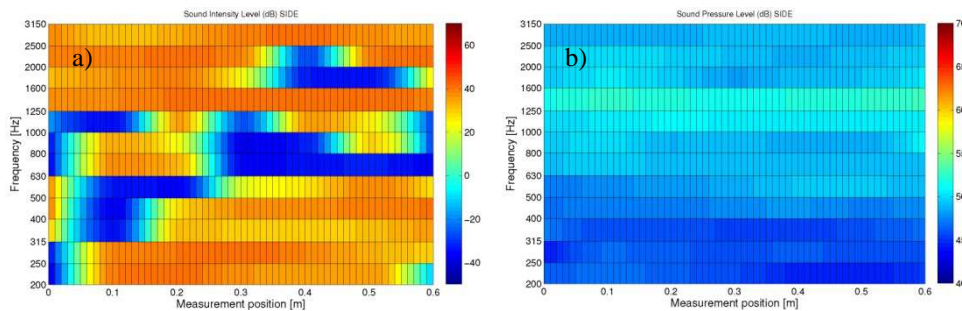

Figure 8 - Livelli di intensità e di pressione sonora (dB) misurati sul lato del campione. La sorgente si trova a sinistra dell'area del grafico - Sound intensity and sound pressure levels (dB) measured on the side of the sample. The source is to the left of the plot areas.
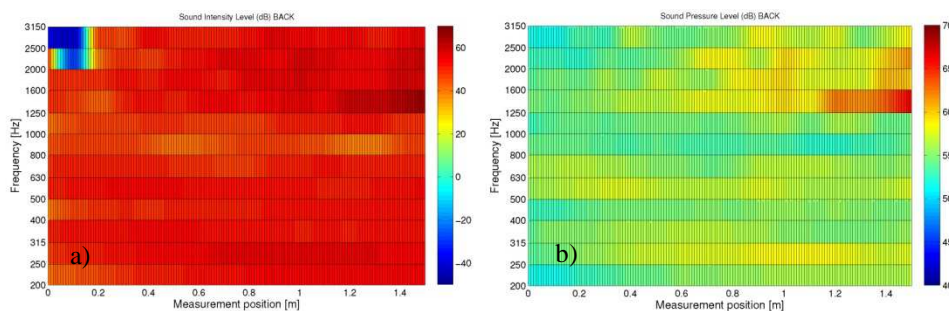

Figure 9 - Livelli di intensità e di pressione sonora (dB) misurati sul retro del campione. La sorgente si trova a destra dell'area del grafico - Sound intensity and sound pressure levels (dB) measured on the rear of the sample. The source is to the right of the plot areas.

Federica Morandi et al.
I cristalli sonici come barriere antirumore
Sonic crystals as tunable noise barriers

The sound intensity levels plot in Fig. 8a show areas with negative values around the first Bragg band gap. The appearance of negative values suggests that the field detected by the intensity probe is severely affected by the out-of-phase noise coming from the surrounding environment, being the front component negligible compared to that. Moving along the side of the sample, these darker regions are concentrated around 800 Hz, with no significant shift in frequency. The sound pressure level (Fig. 8b) is homogeneous with the distance and shows a region of incremented values in the one-third of octave band of 1250 Hz, region which also correspond to high sound intensity levels. This matches perfectly the pattern of the sound field inside the array displayed in Fig. 6b, providing an additional evidence of sound propagation in the longitudinal direction.

Measurements in the rear of the sample were made by shifting the intensity probe parallel to the sample. In this configuration, some regions are detected between the 315 and the 1600 one-third octave bands which display higher sound pressure levels compared to the surrounding areas (Fig. 9b). A band of slightly lower sound intensity level is found between 800 and 1000 Hz, at Bragg frequency. At twice Bragg frequency there is a sudden increase in sound pressure and intensity level at the measurement position closer to the sound source.

3.4 Standardized indices

The measurements conducted so far were aimed at pointing out the multiple scattering process and to detail the sound field distribution inside the sonic crystal. At the University of Bologna the Sound Insulation Index (SI) and the Reflection Index (RI) of sonic crystal noise barriers have been thus measured according to the EN 1793-6 [54] and EN 1793-5 [53] standards, which describe a method which allows to perform laboratory measurements on noise barriers returning results which do not differ significantly from in situ measurements [59]. The width and height of the sample determined the characteristics of a time window that was used to cancel ground reflection and edge diffraction, thus computing the transmitted sound component only, as previously discussed.

The results of the measurements have been presented in detail in Ref. [60], where standardized transmission and reflection measurements for normal incidence are discussed together with measurements performed for diffuse incidence and compared to the performance of other noise barriers. The Sound Insulation index (SI) is computed as:

$$
(7) \qquad SI_j = -10\log\left\{ \frac{1}{n} \sum_{k=1}^{n} \frac{\int_{\Delta f_j} |F[h_{t,k}(t)w_{t,k}(t)]|^2 \, df}{\int_{\Delta f_j} |F[h_{i,k}(t)w_{i,k}(t)]|^2 \, df} \right\} \quad (dB)
$$

where $h_{i,k}(t)$ is the free-field impulse response at the k-th microphone position, $h_{t,k}(t)$ is the impulse response at the k-th microphone position with the barrier in between, $w_{i,k}(t)$ and $w_{t,k}(t)$ are the time windows (Adrienne temporal windows) [54] for the free-field and the transmitted components respectively at the k-th microphone position, F denotes the Fourier transform, j is the index of the j-th one-third octave frequency band, Δf_j is the width of the j-th one-third octave frequency band and n=9 is the number of microphone positions.

Federica Morandi et al.
I cristalli sonici come barriere antirumore
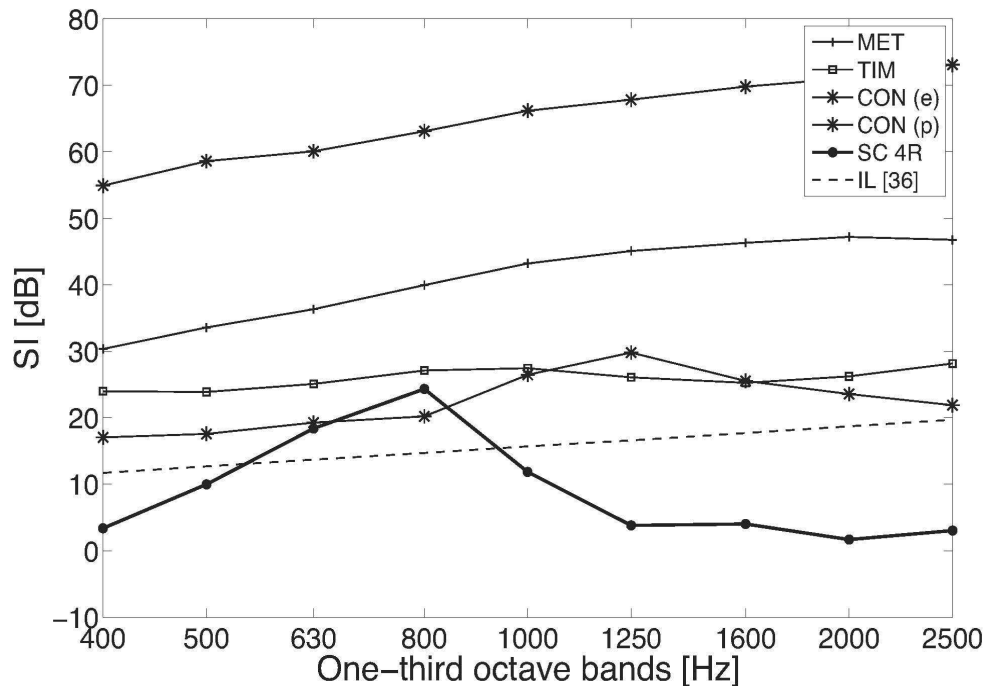**Sonic crystals as tunable noise barriers**

Figure 10 - Confronto fra gli indici SI misurati per un cristallo sonico da 4 file di cilindri (SC, [60]) e per barriere tradizionali [61] - Comparison between the Sound Insulation index measured for a 4-rows sonic crystal (SC, after [60]) and standard noise barriers, after [61].

Figure 10 reports the SI values for lightweight and heavyweight noise barriers existing in the market together with the values measured for sonic crystals. The barriers used for the comparison are taken from Ref. [61]: a metallic non-flat barrier (MET sample n. 7), a timber barrier (TIM sample n. 9) and a concrete barrier (CON sample n. 13), measured across the acoustic element and across the posts. The timber barrier displays sound insulation values which are of the same order of magnitude of the maximum SI measured for a sonic crystal, while the metal and the concrete barriers show higher sound insulation values. For the concrete barrier, the SI values are measured both across the elements (solid line) and the posts (dashed line). For the latter case the SI value drops dramatically, suggesting that the actual sound insulation behind a real road barrier may be severely limited by the sound leakage at the panel-post junction. Fig. 10 also reports the theoretical IL achievable for a given geometry of the barrier due to the top diffraction according to Ref. [62]. The effectiveness of any noise barrier finds its limit in the top edge diffraction: the maximum theoretical value of IL is generally smaller than the insulation performance of noise barriers.

As a consequence, the high sound insulation values that they provide are equally effective if no treatment of the top edge is provided. Sonic crystals achieve this upper limit in the stop-band regions, and thus can be considered valuable alternatives to other acoustic screens, as discussed in [60] relative to other sets of barriers.

Federica Morandi et al.
I cristalli sonici come barriere antirumore
Sonic crystals as tunable noise barriers

Conclusions

This work presented a first literature review on sonic crystals together with the results of an experimental measurement campaign conducted at the University of Bologna. A brief review of the literature highlighted the state of art of the research on the topic, together with the most commonly used investigation methods, both analytical and numerical. The experimental results showed that Insertion Loss in transmission through the sonic crystal can achieve up to 25 dB at Bragg frequency, while the sound field displays a local maximum in reflection. Measurements inside the sonic crystals showed that the pressure field repeats periodically according to the Bloch-Floquet theorem and that, moving away from the source, the decay of the sound pressure field relates to the presence of an evanescent mode. At twice Bragg frequency, a region of constructive interference is spot; the space-frequency distribution of the Insertion Loss spot in the interpolation map inside the crystal match with the results of the sound intensity measurements, suggesting a flow of energy in the longitudinal direction of the lattice in the region immediately after Bragg frequency. Finally, the comparison of standardized Sound Insulation indices measured for sonic crystals and other noise barriers showed that sonic crystals provide an attenuation comparable to the theoretical Insertion Loss limit due to the top edge diffraction. The potential applications for these periodic arrangements are many and exploit the peculiarities of the phenomenon. The selectivity in frequency can be used to prevent the spread of highly tonal components, typical for instance of the machineries in industrial plants. The addition of resonators, of sound absorbing material or of lattice defects allows to extend the band gap in frequency and elect sonic crystals to candidates for the construction of urban barriers. Among the advantages related to the use of this technology, it is worth recalling the limited weight of the structures, which allows to reduce the foundation costs; the free air flow, which also reduces the loads acting on the foundations by reducing the tilting moment due to wind or the shock wave from high speed trains; the continuity of visibility and lightning; finally and not least, a certain aesthetic appeal.

Acknowledgements

Bibliografia

[1]   Kittel, C. (1968). Introduction to Solid State Physics. New York: Wiley.
[2]   Yablonovitch, E. (1987). Inhibited spontaneous emission in solid state physics and electronics. Phys. Rev. Lett. 58 (20), pp. 2059–2062.
[3]   Joannopoulos, J.D., Johnson, S.G., Winn, J.N. and Meade, R.D. (2008). Photonic Crystals: Molding the Flow of Light. Princeton: Princeton University Press.
[4]   Vasseur, J.O., Deymier, P.A., Khelif, A., Lambin, Ph., Djafari-Rouhani, B., Akjouj, A. et al. (2002). Phononic crystal with low filling fraction and absolute acoustic band gap in the audible frequency range: A theoretical and experimental study. Phys. Rev. E 65, 056608.
[5]   Kushwaha, M.S., Halevi, P., Martínez, G., Dobrzynski, L. and Djafari-Rouhani, B. (1994). Theory of acoustic band structure of periodic elastic composites. Phys. Rev. B. 49 (4), pp. 2313-2322.

Federica Morandi et al.
I cristalli sonici come barriere antirumore
Sonic crystals as tunable noise barriers

[6]   Kushwaha, M.S. and Djafari-Rouhani, B. (1998). Sonic stop-bands for periodic arrays of metallic rods: honeycomb structure. J. Sound Vib. 218 (4), pp. 697-709.

[7]   Kafesaki, M. and Economou, E.N. (1999). Multiple-scattering theory for three-dimensional periodic acoustic composites. Phys. Rev. B. 60 (17), pp. 11993-12001.

[8]   Veselago, V.G. (1968). The electrodynamics of substances with simultaneously negative values of ε and μ. Sov. Ohys. Usp. 10, pp. 509-514.

[9]   Pendry, J.B., Holden, A.J., Robbins, D.J. and Stewart, W.J. (1999). Magnetism from conductors and enhanced nonlinear phenomena. IEEE Trans. Microwave Theory Tech. 47 (11), pp. 2075-2084.

[10] Smith, D.R., Padilla, W.J., Vier, D.C., Nemat-Nasser, S.C. and Schultz, S. (2000). Composite medium with simultaneously negative permeability and permittivity. Phys. Rev. Lett. 84 (18), pp. 4184-4187.

[11] Liu, Z., Zhang, X., Mao, Y., Zhu, Y.Y., Yang, Z., Chan, C.T. et al. (2000). Locally resonant sonic materials. Science 289, pp. 1734-1736.

[12] Yang, Z., Dai, H.M., Chan, N.H., Ma, G.C. and Sheng, P. (2010). Acoustic meta-material panels for sound attenuation in the 500-1000 Hz regime. Appl. Phys. Lett. 96, 041906.

[13] Mei, J., Ma, G., Yang, M., Yang, Z., Wen, W. and Sheng, P. (2012). Dark acoustic metamaterials as super absorbers for low-frequency sound. Nat. Comm. 3:756, pp. 1-7.

[14] Fang, N., Xi, D., Xu, J., Ambati, M., Srituravanich, W., Sun, C. et al. (2006). Ultrasonic metamaterials with negative modulus. Nat. Mater. 5, pp. 452-456.

[15] Ding, C., Hao, L. and Zhao, X. (2010). Two-dimensional acoustic metamaterial with negative modulus. J. Appl. Phys. 108, 074911.

[16] Ding, Y., Liu, Z., Qiu, C. and Shi, J. (2007). Metamaterial with simultaneously negative bulk modulus and mass density. Phys. Rev. Lett. 99, 093904.

[17] Li, J. and Chan, C.T. (2004). Double-negative acoustic metamaterial. Phys. Rev. E 70, 055602.

[18] Cheng, Y., Xu, J.Y. and Liu, X.J. (2008). One-dimensional structured ultrasonic metamaterials with simultaneously negative dynamic density and modulus. Phys. Rev. B 77, 045134.

[19] Pendry, J.B., Schurig, D. and Smith, D.R. (2006). Controlling electromagnetic fields. Science 312, pp. 1780-1782.

[20] Schurig, D., Mock, J.J., Justice, B.J., Cummer, S.A., Pendry, J.B., Starr, A.F. et al. (2006). Metamaterial electromagnetic cloak at microwave frequencies. Science 314, pp. 977-979.

[21] Milton, G.W., Briane, M. and Willis, J.R. (2006). On cloaking for elasticity and physical equations with a transformation invariant form. New J. Phys. 8, 248.

[22] Cummer, S.A. and Schurig, D. (2007). One path to acoustic cloaking. New J. Phys. 9, 45.

[23] Chen, H. and Chan, C.T. (2007). Acoustic cloaking in three dimensions using acoustic metamaterials. Appl. Phys. Lett. 91, 183518.

[24] Twersky, V. (1950). Multiple scattering of radiation by an arbitrary configuration of parallel cylinders. J. Acoust. Soc. Am. 24(1), pp. 42-46.

[25] Mártinez-Sala, R., Sancho, J., Sánchez, J.V., Gomez, V., Llinares, J. and Meseguer, F. (1995). Sound attenuation by sculpture. Nature 378 (6554), 241.

[26] Chen, Y.Y. and Ye, Z. (2001). Theoretical analysis of acoustic stop bands in two-dimensional periodic scattering arrays. Phys. Rev. E 64, 036616.

Federica Morandi et al.
I cristalli sonici come barriere antirumore
Sonic crystals as tunable noise barriers

[27] Robertson, W. M. and Rudy, J. F. III (1998). Measurements of acoustic stop band in two-dimensional periodic scattering arrays. J. Acoust. Soc. Am. 104(2), pp. 694-699.

[28] Sánchez-Pérez, J.V., Caballero, D., Mártinez-Sala, R., Rubio, C., Sánchez-Dehesa, J., Meseguer, F. et al. (1998). Sound attenuation by a two-dimensional array of rigid cylinders. Phys. Rev. Lett. 80, pp. 5325-5328.

[29] Sánchez-Pérez, J.V., Rubio, C., Mártinez-Sala, R., Sánchez-Grandia, R. and Gomez, V. (2002). Acoustic barriers based on periodic arrays of scatterers. Appl. Phys. Lett. 81 (27), pp. 5240-5242.

[30] Sanchis, L., Cervera, F., Sánchez-Dehesa, J., Sánchez-Pérez, J.V., Rubio, C. and Martínez-Sala, R. (2001). Reflectance properties of two-dimensional sonic band-gap crystals. J. Acoust. Soc. Am. 109(6), pp. 2598-2605.

[31] Sanchis, L., Hakansson, A., Cervera, F., Sánchez-Dehesa, J. (2003). Acoustic interferometers based on two-dimensional arrays of rigid cylinders in air. Phys. Rev. B 67, 035422.

[32] Pichard, H., Richoux, O. and Groby, J.P. (2012). Experimental demonstrations in audible frequency range of band gap tunability and negative refraction in two-dimensional sonic crystal. J. Acoust. Soc. Am. 132 (4), pp. 2816-2822.

[33] Romero-García, V., Lagarrigue, C., Groby, J.P., Richoux, O. and Tournat, V. (2013). Tunable acoustic waveguides in periodic arrays made of rigid square-rod scatterers: theory and experimental realization. J. Phys. D: Appl. Phys. 46 (30), 305108.

[34] Romero-García, V., Krynkin, A., Garcia-Raffi, L.M., Umnova, O. and Sánchez-Pérez, J.V. (2013). Multi-resonant scatterers in sonic crystals: Locally multi-resonant acoustic metamaterials. J. Sound Vib. 332 (1), pp. 184-198.

[35] Elford, D.P., Chalmers, L., Kusmartsev, F.V. and Swallowe, G.M. (2011). Matryoshka locally resonant sonic crystal. J. Acoust. Soc. Am. 130 (5), pp. 2746-2755.

[36] Krynkin, A., Umnova, O., Chong, A., Taherzadeh, S. and Attenborough, K. (2011). Scattering by coupled resonating elements in air. J. Phys. D: Appl. Phys. 44, 125501.

[37] Umnova, O., Attenborough, K. and Linton, C.M. (2006). Effects of porous covering on sound attenuation by periodic arrays of cylinders", J. Acoust. Soc. Am. 119 (1), pp. 278-284.

[38] Sánchez-Dehesa, J., García-Chocano, V.M., Torrent, D., Cervera, F., Cabrera, S. and Simon, F. (2011). Noise control by sonic crystals barriers made of recycled materials. J. Acoust. Soc. Am. 129 (3), pp. 1173-1183.

[39] García-Chocano, V.M. and Sánchez-Dehesa, J. (2013). Optimum control of broadband noise by arrays of cylindrical units made of a recycled materials. Appl. Acoust. 74, pp. 58-62.

[40] Krynkin, A., Umnova, O., Sánchez-Pérez, J.V., Chong, A.Y.B., Taherzadeh, S. and Attenborough, K. (2011). Acoustic insertion loss due to two dimensional periodic arrays of circular cylinders parallel to a nearby surface. J. Acoust. Soc. Am. 130 (6), pp. 3736-3745.

[41] Martínez-Sala, R., Rubio, C., García-Raffi, L.M., Sánchez-Pérez, J.V., Sánchez-Pérez, E.A. and Llinares, J. (2006). Control of noise by trees arranged like sonic crystals. J. Sound Vib. 291, pp. 100-106.

[42] Lagarrigue, C., Groby, J.P. and Tournat, V. (2013). Sustainable sonic crystal made of resonating bamboo rods. J. Acoust. Soc. Am. 133 (1), pp. 247-254.

[43] Sigalas, M.M. (1998). Defect states of acoustic waves in a two-dimensional lattice of solid cylinders. J. Appl. Phys. 84 (6), pp. 3026-3030.

Federica Morandi et al.
I cristalli sonici come barriere antirumore
Sonic crystals as tunable noise barriers

[44] Wu, L.Y. and Chen, L.W. (2010). Wave propagation in a 2D sonic crystal with a Helmholtz resonant defect. J. Phys. D: Appl. Phys. 43, 055401.

[45] Romero-García, V., Sánchez-Pérez, J.V., García-Raffi, L.M., Herrero, J.M., García-Nieto, S. and Blasco, X. (2009). Hole distribution in phononic crystals: Design and optimization. J. Acoust. Soc. Am. 125 (6), pp. 3774-3783.

[46] Romero-García, V., Sánchez-Pérez, J.V., Castiñeira-Ibáñez, S., Garcia-Raffi, L.M. (2010). Evidences of evanescent Bloch waves in phononic crystals. Appl. Phys. Lett. 96, 124102.

[47] Castineira-Ibánez, S., Rubio, C., Romero-García, V., Sánchez-Pérez, J.V. and García-Raffi, L.M. (2012). Design, manufacture and characterization of an acoustic barrier made of multiphenomena cylindrical scatterers arranged in a fractal-based geometry. Archives of Acoustics 37 (4),pp. 455-462.

[48] EN (2012). EN 1793-2:2012. Road traffic noise reducing devices - Test method for determining the acoustic performance - Part 2: Intrinsic characteristics of airborne sound insulation under diffuse sound field conditions. CEN, Brussels.

[49] Herrero-Durá, I., Picó, R., Sánchez-Morcillo, V., Garcia-Raffi, L.M. and Romero-García, V. (2016). "Vibroacoustic effects of resonant sonic crystals in sound absorption. Proceedings of Euroregio. Porto, 13-15 June.

[50] Linton, C.M. and Evans, D.V. (1990). The interaction of waves with arrays of vertical circular cylinders. J. Fluid Mech. 215, pp. 549-569.

[51] Mei, J., Liu, Z., Shi, J. and Tian, D. (2003). Theory for elastic wave scattering by a two-dimensional periodical array of cylinders: An ideal approach for band-structure cal-culations", Phys. Rev. B. 67, 245107.

[52] Godinho, L., Soares, D.Jr. and Santos, P.G (2016). Efficient analysis of sound propagation in sonic crystals using an ACA-MFS approach. Eng. Anal. Bound. Elem. 69, pp. 72-85.

[53] EN (2014). EN 1793-5:2014. Road traffic noise reducing devices – Test method for determining the acoustic performance - Part 5: Intrinsic characteristics - In situ values of sound reflection under direct sound field conditions. CEN, Brussels.

[54] EN (2012). EN 1793-6:2012. Road traffic noise reducing devices – Test method for determining the acoustic performance - Part 6: Intrinsic characteristics - In situ val-ues of airborne sound insulation under direct sound field conditions. CEN, Brussels.

[55] Sandberg, U. (2003). The multi-coincidence peak around 1000 Hz in tyre/road noise spectra. Proceedings of Euronoise. Naples, 19-21 May.

[56] Garai, M. and Guidorzi, P. (2015). Sound reflection measurements on noise barriers in critical conditions. Building and Environment 94 (2), pp. 752–763.

[57] Morandi, F., Guidorzi, P., Miniaci, M., Marzani, A. and Garai, M. (2015). Acoustic measurements on sonic crystal barriers. Energy Procedia 78, pp. 134-139.

[58] Garai, M., Guidorzi, P. and Morandi, F. (2015). Sound reflection and sound insulation measurement on a sonic crystal noise barrier according to the new European methodology. Proceedings of Internoise. San Francisco, 9-12 August.

[59] Garai, M. and Guidorzi, P. (2000). European methodology for testing the airborne sound insulation characteristics of noise barriers in situ: Experimental verification and comparison with laboratory data. J. Acoust. Soc. Am. 108 (3), pp. 1054-1067.

[60] Morandi, F., Miniaci, M., Marzani, A., Barbaresi, L. and Garai, M. (2016). Standardised acoustic characterisation of sonic crystals noise barriers: sound insulation and reflection properties. Appl. Acoust. 114, pp. 294-306.

Federica Morandi et al.
I cristalli sonici come barriere antirumore
Sonic crystals as tunable noise barriers

[61] Garai, M., Schoen, E., Behler, G., Bragado, B., Chudalla, M., Conter, M. et al. (2014). Repeatability and reproducibility of measurements of sound reflection and airborne sound insulation index of noise barriers. Acta Acustica united with Acustica 100 (6), pp. 1186-1201.

[62] Kurze, U.J. and Anderson, G.S. (1971). Sound attenuation by barriers. Appl. Acoust. 4, pp. 35-53.